J Mol Model (2014) 20:2547
DOI 10.1007/s00894-014-2547-3

ORIGINAL PAPER

How does the increment of hetero-cyclic conjugated moieties affect electro-optical and charge transport properties of novel naphtha-difuran derivatives? A computational approach

Aijaz Rasool Chaudhry · R. Ahmed · Ahmad Irfan · Shabbir Muhammad · A. Shaari · Abdullah G. Al-Sehemi

Received: 20 September 2014 / Accepted: 24 November 2014 / Published online: 12 December 2014

Abstract We have investigated computationally the effects of π-conjugation extension on naphtha[2,1-b:6,5-b'] difuran (DPNDF); where we increase the number of fused NDF (central core) and furan rings in the parent molecule. The molecular structures of all analogues have been optimized at the ground (S_0) and first excited (S_1) states using density functional theory (DFT) and time-dependent density functional theory (TD-DFT), respectively. Then highest occupied molecular orbitals (HOMOs), the lowest unoccupied molecular orbitals (LUMOs), photophysical properties, adiabatic/vertical electron affinities (EAa)/(EAv), adiabatic/vertical ionization potentials (IPa)/(IPv), and hole/electron reorganization energies λ_h/λ_e have been investigated. The effect of NDF and furan rings on structural and electro-optical properties has also been studied. Our calculated reorganization energies of 1a, 1b, and 2c reveal them, materials with balanced hole/electron charge transport, whereas 2a and 2b are good hole-transport materials. By increasing the number of furan rings; the photostability was augmented in 2a, 2b, and 2c.

Keywords Electro-optical properties · Hetero-cyclic conjugation · Organic semiconductor materials · Electronic materials

A. R. Chaudhry · R. Ahmed (✉) · A. Shaari
Department of Physics, Faculty of Science, Universiti Teknologi Malaysia, UTM Skudai, Johor 81310, Malaysia
e-mail: rashidahmed@utm.my

A. R. Chaudhry (✉) · S. Muhammad
Department of Physics, Faculty of Science, King Khalid University, P.O. Box 9004, Abha 61413, Saudi Arabia
e-mail: aijaz_bwp27@hotmail.com

A. Irfan · A. G. Al-Sehemi
Department of Chemistry, Faculty of Science, King Khalid University, P.O. Box 9004, Abha 61413, Saudi Arabia

A. G. Al-Sehemi
Unit of Science and Technology, Faculty of Science, King Khalid University, P.O. Box 9004, Abha 61413, Saudi Arabia

A. R. Chaudhry · A. Irfan · S. Muhammad · A. G. Al-Sehemi
Center of Excellence for Advanced Materials Research, King Khalid University, P.O. Box 9004, Abha 61413, Saudi Arabia

Introduction

π-conjugation contributes a considerable role in designing the structural, optoelectronic, and charge transfer properties of organic semiconductor materials (OSMs) [1–6]. For the past decades, significant attention has been dedicated to the construction of π-conjugated novel systems [7–13] due to their potential applications in optoelectronics devices. π-conjugated OSMs are of immense interest for experimental and theoretical researchers due to their bendable displays, low fabrication cost, low weight and flexible substrates [14–22]. These give organic materials (OMs) a huge advantage over conventional inorganic silicon-based transistors for semiconducting behavior. Since first reported in 1986 OSMs are intensively investigated for their applications in optoelectronic devices and microelectronics, such as organic field-effect transistors (OFETs) [23–27], organic light-emitting transistors (OLETs) [28], organic light-emitting diodes (OLEDs) [29–31] and organic photo-voltaic devices (OPVs) [30, 32, 33].

In OSMs, many experimental and theoretical researchers had focused on thiophene [34–50] containing OMs as compared to furan containing OMs [51–54] for use in OFETs and OLEDs. During the last few years more attention has been given to furan as basic building block for organic π-conjugated materials, because furan containing OMs are more stable and potentially applicable in OFETs and OLEDs [55,

56, 28, 57–60]. Binaphtha-furanyl has been reported to be a good OLETs [28] material and furan based materials were considered by the same researchers to have great potential as a versatile organic semiconductor, especially in light of their distinct photophysical properties in solid state compared to their thiophene counterpart, making them a new material class applicable to OFET, OLETs and OPVs. Recently naphtha[2,1-b:6,5-b']difuran (DPNDF) and its derivative were experimentally synthesized for solution-processed single-crystal OFET with high hole mobility [61]. The effect of the furan rings in π-conjugation organic electronic materials was experimentally and theoretically studied in relation to their electrochemical and optical properties and concluded; these new compounds present consistent electronic properties compatible for application in organic electronics [11]. Naphthalimide-fused derivatives have been synthesized and characterized for n-type and ambipolar charge transport materials in OFET [62]. The influence of conjugation on electronic and structural properties has been studied experimentally as well as theoretically. In our previous study [63], it was found that the furan may be a good electron transport material with very low reorganization energy for electron λ(e). Moreover using the experimental crystal of DPNDF [61] as a starting point we studied the effect of electron withdrawing groups (EWGs) [64, 65] and heteroatom substitution [66]. The influence of push-pull strategies has been studied as well [67].

In the present study we extend our work to investigate the effects of π-conjugation elongation on the structural, electronic, photophysical, and charge transfer properties. For this purpose five new derivatives were designed from the same parent molecule of DPNDF [61] by increasing the number of naphtha-difuran (NDF); named as 1a and 1b, respectively, where we increase the number of fused NDF rings (central core) in the parent molecule. For 2a, 2b, and 2c the number of furan rings have been increased; see Fig. 1 for schematic diagram of derived systems.

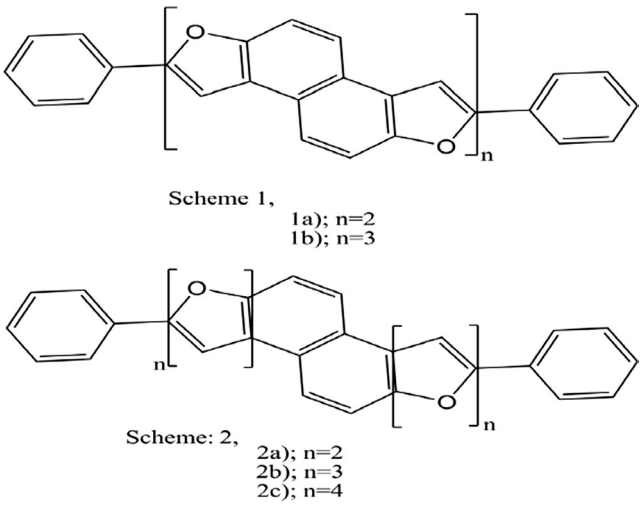

Fig. 1 Schematic diagram of derivatives with labeling

We optimized the geometries of these structures at both ground and excited states and compared the results to see the effect of conjugation length on the molecular structures. Along with the comparative study, the structural, electronic, photophysical, and charge transfer properties of these analogues such as highest occupied molecular orbitals (E_{HOMO}), lowest unoccupied molecular orbitals (E_{LUMO}), HOMO-LUMO energy gap (E_g), reorganization energies for hole (λ_h) and electron (λ_e), ionization potentials (IPs), and electron affinities (EAs) have been calculated by computational methods and discussed in detail. Photostability has been discussed on the bases of molecular electrostatic potentials (MEP). The computational results of these analogues have been compared with experimental data where available.

Computational details

Density functional theory (DFT) has been used to optimize the initial molecular structures at the ground states (S_0) by applying the hybrid exchange correlation functional B3LYP [68, 69] with 6-31G** basis sets [70–72]. For excited states (S_1) time-dependent density functional theory (TD-DFT) through the hybrid functional TD-B3LYP [73–78] with the same basis set was used to optimize the geometries of all the derivatives. Electronic, photophysical properties including wavelengths of maximum absorption (λ_{abs}) and emission (λ_{emis}) have been calculated at the same level of theory.

The reorganization energy (λ) represents the geometric relaxation energy of a molecule from charged to the neutral state [79, 80], and from the neutral to charged state. These two terms are calculated directly from the adiabatic potential

Table 1 Calculated optimized bond lengths (Å) and bond/dihedral angles in degree at the B3LYP/6-31G** and TD-B3LYP/6-31G** levels of theory at ground (S_0) state and excited (S_1) state (in brackets)

Bond lengths	1a	1b	2a	2b	2c
O-C	1.39 (1.39)	1.39 (1.38)	1.39 (1.39)	1.39 (1.39)	1.39 (1.39)
C-O	1.37 (1.36)	1.37 (1.37)	1.37 (1.39)	1.37 (1.39)	1.37 (1.39)
NDF-phenyl	1.45 (1.44)	1.45 (1.45)	1.45 (1.43)	1.45 (1.44)	1.45 (1.44)
C-O-C	106.84 (107.04)	106.84 (106.97)	105.79 (105.77)	105.86 (105.84)	105.87 (105.88)
O-C-C	116.64 (117.06)	116.65 (116.85)	116.51 (116.95)	116.36 (116.77)	116.36 (116.08)
C-O-C-C	179.99 (179.99)	179.99 (179.99)	179.99 (179.99)	180.00 (180.00)	179.97 (180.00)
O-C-C-C	179.89 (179.96)	179.94 (179.97)	179.99 (179.98)	179.96 (179.97)	179.92 (179.96)

energy surfaces for λ_h and λ_e [81–83]. The reorganization energy for hole (λ_h) was evaluated as:

$$\lambda_h = \left[E^1(R)^+ - E(\text{cation})\right] + \left[E^1(R) - E(\text{neutral})\right] \quad (1)$$

$E^1(R)$ is the energy of neutral at the optimized charged (cation) species, and $E^1(R)^+$ is energy of the charge (cation) at the geometry of the optimized neutral species.

The reorganization energy for electron (λ_e) was evaluated as:

$$\lambda_e = \left[E^1(R)^- - E(\text{anion})\right] + \left[E^1(R) - E(\text{neutral})\right], \quad (2)$$

$E^1(R)$ is the energy of neutral molecule at the geometry of the optimized charged (anion) species, and $E^1(R)^-$ is energy of the charged (anion) species at the geometry of the optimized neutral species. These reorganization energies for hole as well as electron were calculated using B3LYP/6-31G** level of theory for all the derivatives.

The IPs and EAs can be either for adiabatic excitations (a), optimized structure for both the neutral and charge molecule or vertical excitation (v), at the geometry of the neutral molecule. The adiabatic and vertical ionization potential (IPa and IPv); electron affinity (EAa and EAv) have been calculated at the B3LYP/6-31G** level of theory as follows:

$$\text{IPa} = E(\text{cation}) - E(\text{neutral}) \text{ and} \quad (3)$$
$$\text{IPv} = E^1(R)^+ - E(\text{neutral})$$

$$\text{EAa} = E(\text{neutral}) - E(\text{anion}) \text{ and} \quad (4)$$
$$\text{EAv} = E(\text{neutral}) - E^1(R)^-,$$

where $E^1(R)^+$ and $E^1(R)^-$ correspond to the energies of charged (cation and anion) states at the optimized geometry

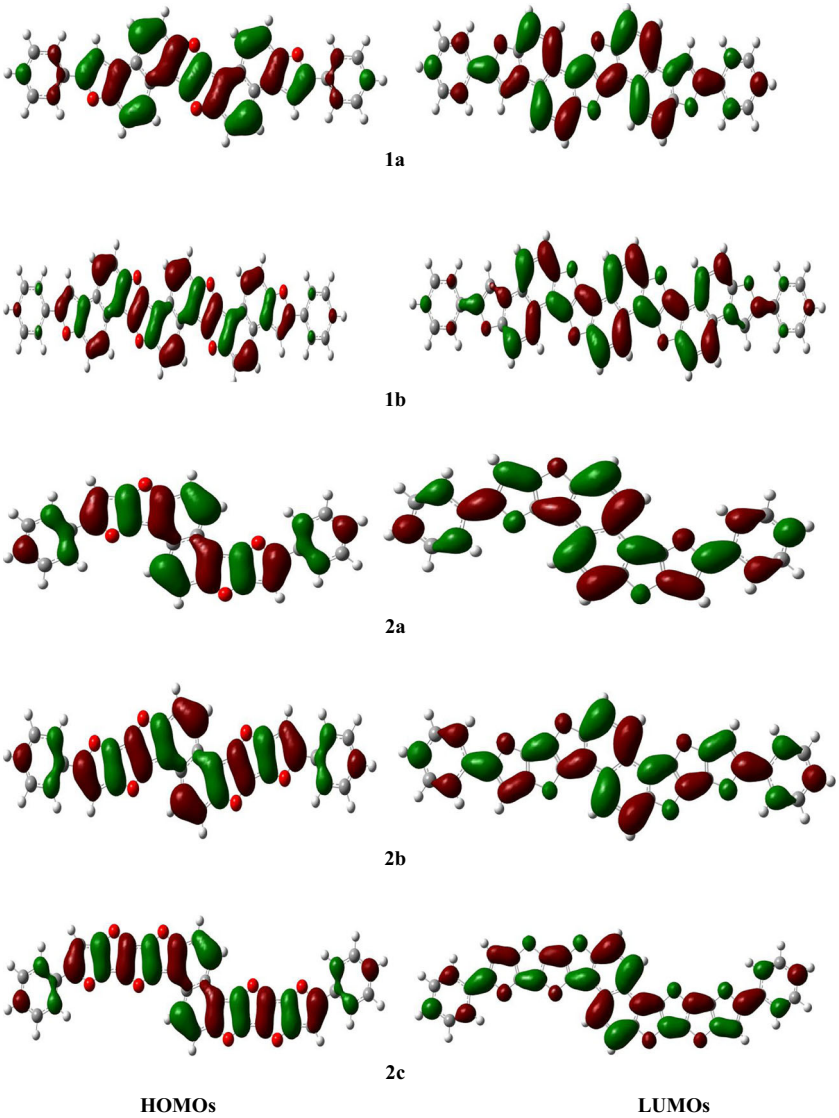

Fig. 2 Distribution patterns of HOMOs and LUMOs at ground state for all derivatives

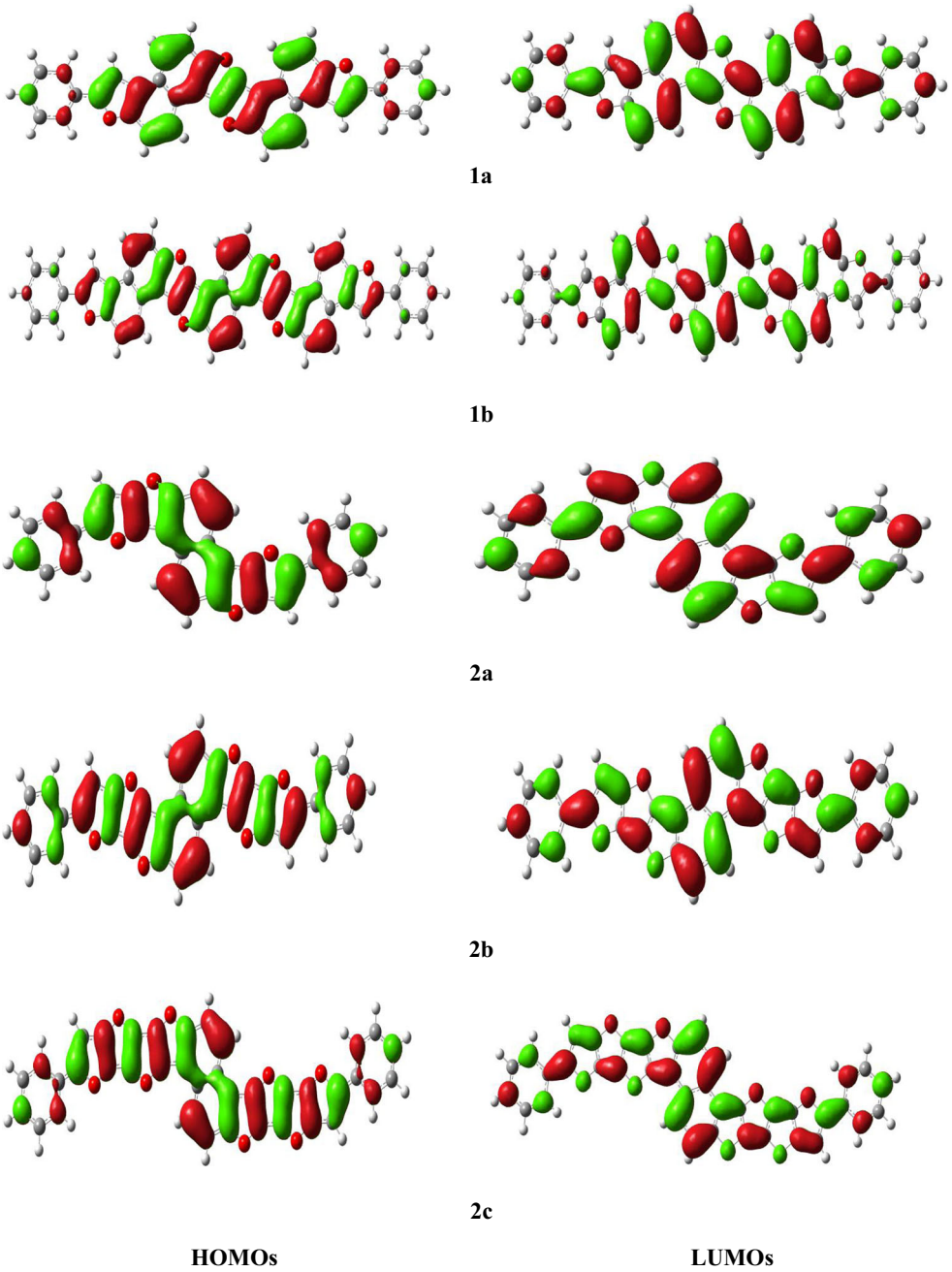

Fig. 3 Distribution patterns of HOMOs and LUMOs at excited state for all derivatives

of the neutral molecule, respectively. All first-principles calculations were carried out using Gaussian 09 package [84].

Results and discussion

Ground and excited states geometries

The optimized bond lengths and bond/dihedral angles for the investigated derivatives at ground S_0 and excited S_1 states (in brackets) have been tabulated in Table 1, respectively. As shown in Table 1 from ground S_0 to excited S_1 state, the bond

Table 2 The E_{HOMO}, E_{LUMO}, and E_g for S_0 states/S_1 states (in the brackets) at the B3LYP/6-31G** and TD-B3LYP/6-31G** levels of theory

	1a	1b	2a	2b	2c
E_{HOMO} (eV)[a]	−4.99 (−4.81)	−4.96 (−4.80)	−4.93 (−4.74)	−4.82 (−4.65)	−4.75 (−4.58)
E_{LUMO} (eV)	−1.67 (−1.87)	−1.78 (−1.96)	−1.66 (−1.88)	−1.72 (−1.92)	−1.79 (−1.97)
E_g (eV)	3.32 (2.94)	3.18 (2.84)	3.27 (2.87)	3.10 (2.73)	2.96 (2.61)

[a]: Computed values for comparison from ref. [65]

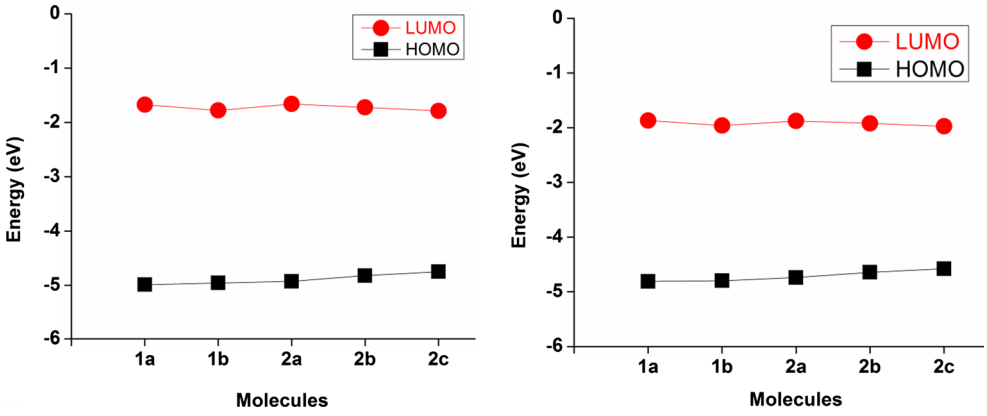

Fig. 4 Comparison of E_{HOMO} and E_{LUMO} for ground (S_0) state (left)/excited (S_1) state (right) at the B3LYP/6-31G** and TD-B3LYP/6-31G** levels of theory

lengths and bond/dihedral angles have not increased or decreased significantly. All the derivatives are densely packed, which restrict the bond lengths and bond/dihedral angles from shortening and lengthening.

Electronic properties

Frontier molecular orbitals (ground and excited states)

The distribution patterns of HOMOs and LUMOs for all the molecules at ground (S_0) and excited (S_1) states are shown in Fig. 2 and Fig. 3, respectively; evaluated at B3LYP/6-31G** and TD-B3LYP/6-31G** levels of theory. At S_0 state for **1a**, **1b**, **2a**, **2b**, and **2c** the HOMO formation has been following the same trend as the charge delocalized on all backbone, whereas charge is localized (lone-pair) on the outer phenyl ring. The oxygen atoms are not taking part in formation of HOMO. For LUMO formation the delocalization of charge has been found on the central core for all molecules. The charge has been localized on all oxygen atoms. All the molecules have been found with similar patterns of the LUMO formation.

At S_1 state, in the formation of HOMO, it was found that the charge has been delocalized on all backbone; the oxygen atoms are not involved in formation of HOMO. For LUMO formation all the derivatives have been found with similar patterns of the LUMO formation, where the charge has been delocalized on the central NDF and furan rings for all the molecules.

The energies of HOMOs (E_{HOMO}), LUMOs (E_{LUMO}), and HOMO-LUMO energy gaps (E_g) at ground states for all the molecules have been tabulated in Table 2. The graphical representation of E_{HOMO} and E_{LUMO} is shown in Fig. 4 (left) for more clear understanding of the E_g at ground state. The E_{HOMO} of studied molecules **1a**, **1b**, **2a**, **2b**, and **2c** are −4.99, −4.96, −4.93, −4.82, and −4.75 eV, respectively. The trend of E_{HOMO} is **1a** (−4.99 eV)<**1b** (−4.96 eV)<**2a** (−4.93 eV)<**2b** (−4.82 eV)<**2c** (−4.75 eV) and of E_{LUMO} is **2c** (−1.79 eV)>**1b** (−1.78 eV)>**2b** (−1.72 eV)>**1a** (−1.67 eV)>**2a** (−1.66 eV). The computed E_{HOMO} of all the molecules has been decreased as compared to the experimental value [61] of parent molecule DPNDF, and are in a healthy agreement with the computed values of E_{HOMO} (−5.10 eV) [65] of the same molecule DPNDF. Similarly the E_{LUMO} for all the molecules has been decreased as compared to the already computed value of parent molecule [65].

The trend in the E_g is **1a** (3.32 eV)>**2a** (3.27 eV)>**1b** (3.18 eV)>**2b** (3.10 eV)>**2c** (2.96 eV). It can be seen from Table 2 that the E_{LUMO} has been enhanced by increasing the number of NDF and furan rings in the parent molecule which would increase the electron injection barrier resulting in reduced electron injection. It is expected that new molecules might be good hole transport materials.

The E_{HOMO}, E_{LUMO}, and E_g at excited states for all the molecules have been presented in Table 2 (in the bracket). The graphical comparison of E_{HOMO} and E_{LUMO} is given in Fig. 4 (right) for more clear representation of E_g. The trend of

Table 3 Calculated wavelengths in nm for maximum absorption (λ_{abs}), emission (λ_{emis}), oscillator strength (f), and contribution of HOMO to LUMO for S_0 and S_1 states[a]

	λ_{abs}	f	Contribution	λ_{emis}	f	Contribution
1a	420	1.56	HOMO→LUMO (98 %)	469	1.69	HOMO→LUMO (99 %)
1b	443	2.06	HOMO→LUMO (97 %)	494	2.16	HOMO→LUMO (99 %)
2a	422	1.22	HOMO→LUMO (99 %)	474	1.32	HOMO→LUMO (100 %)
2b	445	1.80	HOMO→LUMO (99 %)	500	1.94	HOMO→LUMO (100 %)
2c	468	2.03	HOMO→LUMO (99 %)	526	2.17	HOMO→LUMO (100 %)

[a]: Computed values (λ_{abs}=381 nm; λ_{emis}=427 nm) for comparison with ref. [65]

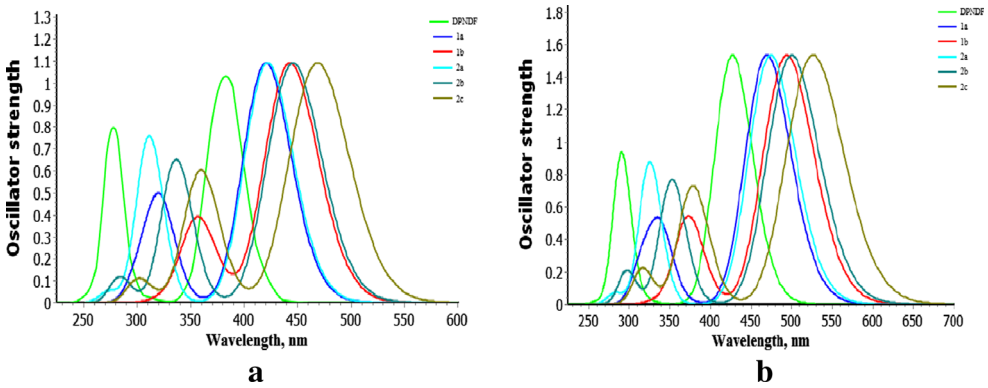

Fig. 5 (**a**) computed absorption spectra (**b**) computed emission spectra, at the TD-DFT level

E_{HOMO} is **1a** (−4.81 eV)>**1b** (−4.80 eV)>**2a** (−4.74 eV)>**2b** (−4.65 eV)>**2c** (−4.58 eV), respectively. The trend of E_{LUMO} is **2c** (−1.97 eV)>**1b** (−1.96 eV)>**2b** (−1.92 eV)>**2a** (−1.88 eV)>**1a** (−1.87 eV), respectively, whereas the trend in the E_g is **1a** (2.94 eV)>**2a** (2.87 eV)>**1b** (2.84 eV)>**2b** (2.73 eV)>**2c** (2.61 eV). It has been observed that E_{HOMO} and E_{LUMO} have been reduced with increase in the number of NDF and furan rings. So we predict the red shifted emission wavelengths for all the molecules.

Photophysical properties

Oscillator strengths (f), λ_{abs}, λ_{emis}, and HOMO-LUMO contribution have been evaluated and tabulated in Table 3. The computed absorption and emission spectra, at the TD-DFT level are graphically shown in Fig. 5 (a) and (b), respectively. Table 3 shows the maximum HOMO→LUMO contribution at the ground states (S_0). The major contribution at ground state for **1a** is HOMO→LUMO (98 %) while for **1b** is from HOMO→LUMO (97 %), whereas for **2a**, **2b**, and **2c** is from HOMO→LUMO (100 %). Similarly the maximum contribution of HOMOs to LUMOs for excited states is from HOMO→LUMO (99 %) for **1a** and **1b**, whereas from HOMO→LUMO (100 %) for **2a**, **2b**, and **2c**. The λ_{abs} have the red shift of 39 nm, 62 nm, 41 nm, 64 nm, and 87 nm for **1a**, **1b**, **2a**, **2b**, and **2c**, respectively, whereas the λ_{emis} also have the red shift of 42 nm, 67 nm, 47 nm, 73 nm, and 99 nm for **1a**, **1b**, **2a**, **2b**, and **2c**, respectively as compared to the parent molecule of DPNDF [65]. The emission wavelengths have been amplified toward red shift for all the molecules with increase in the NDF and furan rings in the central core of DPNDF as compared to the computed values of parent molecule DPNDF [65]. Structure–property relationship revealed that by enlarging the central core, the λ_{abs} and the λ_{emis} have shown red shifted behavior for **1a**, **1b**, **2a**, **2b**, and **2c** as shown in Fig. 5.

Charge transfer properties

Electron affinity (EA) and ionization potential (IP) are the most important properties to calculate the charge injection barriers, which have been evaluated at the B3LYP/6-31G** level. The adiabatic/vertical IP (IPa/IPv) and adiabatic/vertical EA (EAa/EAv) of these molecules have been calculated and tabulated in Table 4. A graphical comparison of the IPv (χ) and EAv has been drawn in Fig. 6 (left) to represent the results more clearly. In organic semiconductor materials increasing the injection ability for hole and electron lower IP and higher EA is very crucial. In OFETs the organic materials having high EAv might be better for n-type and of small IPv might favor p-type charge injection [85]. From Table 4 it is clear that **1a**, **1b**, **2a**, **2b**, and **2c** have the EAv 0.66, 0.88, 0.53, 0.69, and 0.82 eV, respectively, which are higher than that of DPNDF [65] computed at the same level of theory. The EAv follow the same trend as for E_{LUMO} for all molecules as it has been observed that the molecule with high LUMO energy has the higher EAv. It can be seen from Table 4 that EAv for studied systems improved by increasing the number of NDF and furan rings in the central core of parent molecule DPNDF.

The reorganization energy is the quantity which is most important for estimating the ability to carry the charge in solids [86, 87]. The reorganization energies at the B3LYP/6-31G** level for electron λ (e) and for hole λ (h) have been given in Table 4. A graphical representation of hole λ (h) and λ (e) has been given in Fig. 6 (right) at the same level of theory to reveal the tendency more clearly. The calculated λ (h) of the **2a** (0.17 eV) at B3LYP/6-31G** level of theory is in good agreement with previously computed value for the parent

Table 4 The vertical/adiabatic ionization potential and electron affinity, the reorganization energy for hole λ(h) and for electron λ(e) at the B3LYP/6-31G** level of theory. All values in eV

	1a	1b	2a	2b	2c
IP (vertical)	6.05	5.88	6.10	5.89	5.75
IP (adiabatic)	5.89	5.82	6.01	5.81	5.68
EA (vertical)	0.66	0.88	0.53	0.69	0.82
EA (adiabatic)	0.73	0.94	0.63	0.78	0.90
λ(h)	0.14	0.10	0.17	0.16	0.15
λ(e)	0.16	0.12	0.20	0.19	0.17

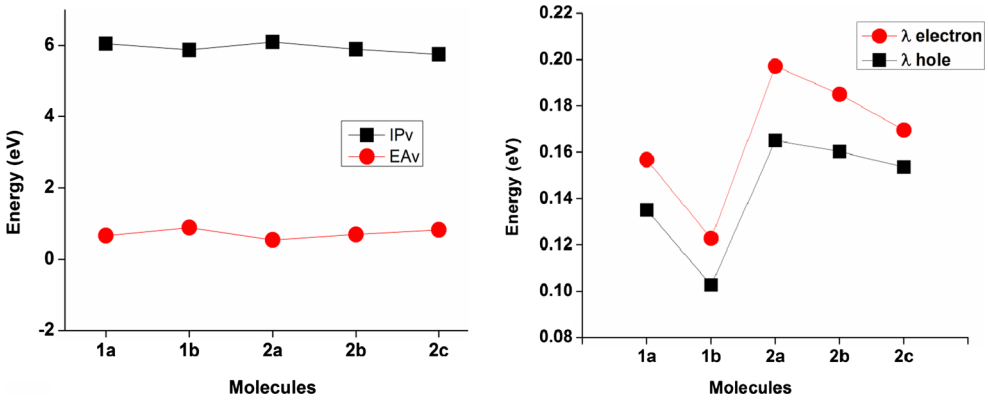

Fig. 6 Graphical representation of IPv and EAv (left); λ(h) and λ(e) (right) calculated at the B3LYP/6-31G** level of theory

molecule DPNDF [61]. Moreover, the computed λ (h) is slightly smaller than λ (e) for all the molecules revealing that they would be better as hole transfer material while giving good agreement with the finding of reference [61]. From Table 4 it is clear that **1a**, **1b**, and **2c** have almost balanced λ (h) and λ (e), so they might be good candidates for hole as well as electron transport materials whereas the molecules **2a** and **2b** have the λ(h) (0.17 and 0.16 eV), which is lower than λ(e) (0.20 and 0.19 eV), respectively. It is predicted that **1a**, **1b**, and **2c** are better for hole as well as electron transport whereas **2a** and **2b** are good hole-transport materials, respectively. The λ(h) for **1a**, **1b**, **2a**, **2b**, and **2c** have been evaluated as 0.14, 0.10, 0.17, 0.16, and 0.15 eV, respectively, at the B3LYP/6-31G** level. These values of λ (h) for all molecules are smaller than that of thiophene based analogue DPNDT (0.19 eV) [88], α-oligofurans (0.23 eV) [89] and naphtho-dithiophene 0.25 eV [90], hence supporting our prediction that these materials would be better as hole carrier transporter than DPNDT, α-oligofurans and naphtho-dithiophene. Moreover, the values λ(e) for all **1a**, **1b**, **2a**, **2b**, and **2c** have been evaluated as 0.16, 0.12, 0.20, 0.19, and 0.17 eV, respectively, which are smaller than naphtho-dithiophene 0.34 eV [90] and oligofuran 0.40 eV [89], revealed that the new designed molecules might be efficient as electron transporter as compared to the naphtho-dithiophene and oligofuran.

Molecular electrostatic potentials

Molecular electrostatic potentials (MEP) have been mapped for all molecules as shown in Fig. 7. Higher negative and positive potential regions are shown in pink and green colors, respectively. The maximum negative regions are favorable for electrophilic attack, whereas maximum positive regions are favorable for nucleophilic attack. The MEP is a real physical observable property, that can be attained experimentally by diffraction methods [91, 92] as well as computationally. MEP represents the complete nuclear and electronic charge distribution of a molecule and is a very useful property to study the reactivity of the given molecule [93–95]. We observed that in all the molecules the high negative potential is distributed on oxygen atoms only, which might be due to the presence of

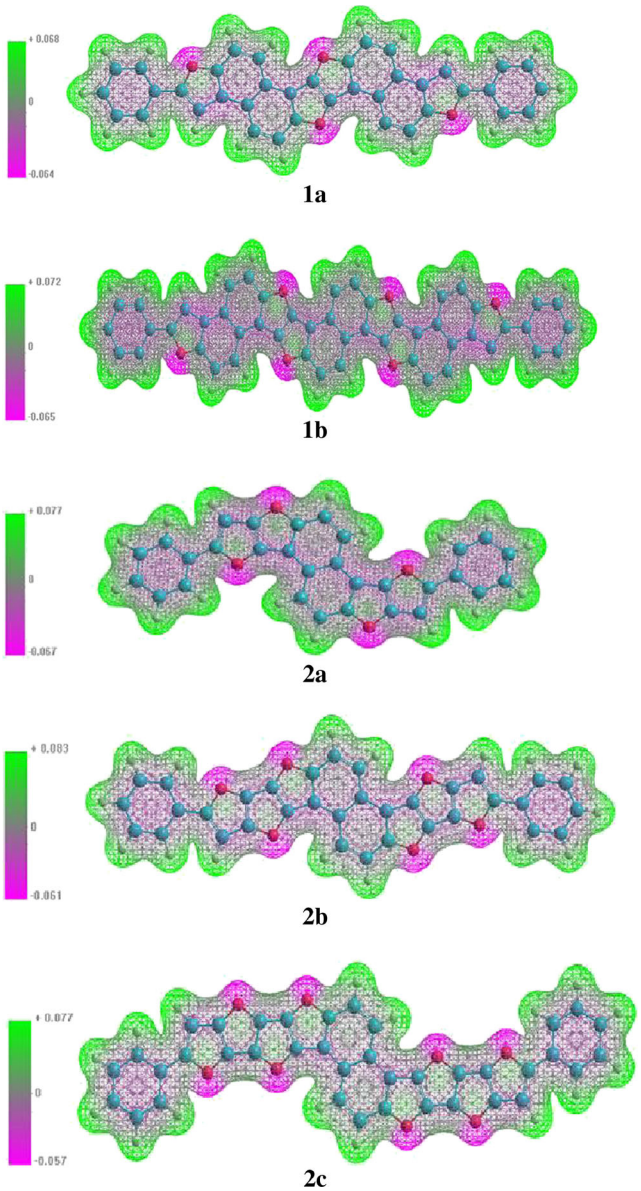

Fig. 7 Molecular electrostatic potential distributions of all the derivatives

lone pairs on oxygen atoms (see Fig. 7). By increasing the number of furan rings; the MEP have been augmented in **2a**, **2b**, and **2c**. Previously, the photostability of organic materials was explained on the basis of MEP [96]. Recently, we pointed out that greater negative potential distributed on the system would enhance the photostability [97]. The higher negative electrostatic potential distribution on the surface will make the oxidation more difficult and resist against the degradation of the molecule (due to the oxidation and photoreactions) [96, 97]. Higher negative electrostatic potential in 2a, 2b, and 2c would decrease the oxidation resulting in the development of photostability which is in good agreement with our previous study.

Conclusions

The HOMOs and LUMOs in all the studied molecules have been delocalized as well as localized throughout the backbone. The E_{HOMO} of all molecules were decreased as compared to the experimental values. By increasing the NDF and furan rings in the central core of the parent molecule, the HOMO energies of all the studied systems have been reduced. The wavelengths of maximum absorption and emission showed the red shifted behavior for all the molecules as compared to the computed value of parent molecule DPNDF. The vertical electron affinity for these molecules was improved by increasing the number of NDF and furan rings in the central core of parent molecule DPNDF. In terms of reorganization energies **1a**, **1b**, and **2c** may be material with balanced hole/electron charge transport. It is predicted that they are better for hole as well as electron transport whereas **2a** and **2b** are good hole-transport materials. By increasing the number of furan rings, the photostability is augmented in **2a**, **2b**, and **2c**. It is predicted that increasing the number of NDF and furan rings in furan based materials might improve the charge injection in all studied systems. It is expected that these materials would be better as OFETs, OLETs, and OLEDs.

Acknowledgments Authors are grateful to the Ministry of the Education/Universiti Teknologi Malaysia (UTM) for providing funding via project Q.J130000.2526.06H15 for the successful execution of this project and the King Khalid University (KKU) for providing the support and facilities to complete this research study.

References

1. Reshak AH, Stys D, Auluck S, Kityk IV (2010) Density functional calculations of the electronic structure of 3-phenylamino-4-phenyl-1, 2,4-triazole-5-thione. Phys Chem Phys 12(12):2975–2980
2. Reshak AH, Stys D, Auluck S, Kityk IV (2009) Ab initio calculation of the electronic band structure, density of states and optical properties of α-2-methyl-1-nitroisothiourea. J Phys Chem B 113(38):12648–12654
3. Reshak AH, Stys D, Auluck S, Kityk IV (2010) Linear and nonlinear optical susceptibilities of 3-phenylamino-4-phenyl-1,2,4-triazole-5-thione. J Phys Chem B 114(5):1815–1821
4. Pokladko M, Gondek E, Sanetra J, Nizioł J, Danel A, Kityk IV, Reshak AH (2009) Spectral emission properties of 4-aryloxy-3-methyl-1-phenyl-1H-pyrazolo[3,4-b]quinolines. Spectrochim Acta A Mol Biomol Spectrosc 73(2):281–285
5. Fuks-Janczarek I, Reshak AH, Kuźnik W, Kityk IV, Gabański R, Lapkowski M, Motyka R, Suwiński J (2009) UV–vis absorption spectra of 1,4-dialkoxy-2,5-bis[2-(thien-2-yl)ethenyl]benzenes. Spectrochim Acta A Mol Biomol Spectrosc 72(2):394–398
6. Wojciechowski A, Ozga K, Reshak AH, Miedzinski R, Kityk IV, Berdowski J, Tylczyński Z (2010) Photoinduced effects in l-alanine crystals. Mater Lett 64(18):1957–1959
7. Matsumi N, Naka K, Chujo Y (1998) Extension of π-conjugation length via the vacant p-orbital of the boron atom. Synthesis of novel electron deficient π-conjugated systems by hydroboration polymerization and their blue light emission. J Am Chem Soc 120(20):5112–5113
8. Morley JO, Docherty VJ, Pugh D (1987) Non-linear optical properties of organic molecules. Part 2 effect of conjugation length and molecular volume on the calculated hyperpolarisabilities of polyphenyls and polyenes. J Chem Soc Perkin Trans 2(9):1351–1355
9. Monkman AP, Burrows HD, Hamblett I, Navarathnam S, Svensson M, Andersson MR (2001) The effect of conjugation length on triplet energies, electron delocalization and electron–electron correlation in soluble polythiophenes. J Chem Phys 115(19):9046–9049
10. Meier H, Stalmach U, Kolshorn H (1997) Effective conjugation length and UV/vis spectra of oligomers. Acta Polym 48(9):379–384
11. Moussallem C, Gohier F, Mallet C, Allain M, Frère P (2012) Extended benzodifuran–furan derivatives as example of π-conjugated materials obtained from sustainable approach. Tetrahedron 68(41):8617–8621
12. Kim R, Amegadze PSK, Kang I, Yun H-J, Noh Y-Y, Kwon S-K, Kim Y-H (2013) High-mobility Air-stable naphthalene diimide-based copolymer containing extended π-conjugation for n-channel organic field effect transistors. Adv Funct Mater 23(46):5719–5727
13. Oldham WJ, Miao Y-J, Lachicotte RJ, Bazan GC (1998) Stilbenoid dimers: effect of conjugation length and relative chromophore orientation. J Am Chem Soc 120(2):419–420
14. Reshak AH, Kamarudin H, Auluck S (2013) Electronic structure, density of electronic states, and the chemical bonding properties of 2, 4-dihydroxyl hydrazone crystals (C13H11N3O4). J Mater Sci 48(10):3805–3811
15. Reshak AH, Kamarudin H, Kityk IV, Auluck S (2013) Electronic structure, charge density, and chemical bonding properties of C11H8N2O o-methoxydicyanovinylbenzene (DIVA) single crystal. J Mater Sci 48(15):5157–5162
16. Reshak AH, Kamarudin H, Auluck S (2012) Acentric nonlinear optical 2,4-dihydroxyl hydrazone isomorphic crystals with large linear nonlinear optical susceptibilities and hyperpolarizability. J Phys Chem B 116(15):4677–4683
17. Reshak AH, Auluck S, Stys D, Kityk IV, Kamarudin H, Berdowski J, Tylczynski Z (2011) Dispersion of linear and non-linear optical susceptibilities for amino acid 2-aminopropanoic CH3CH(NH2)COOH single crystals: experimental and theoretical investigations. J Mater Chem 21(43):17219–17228
18. Reshak AH, Stys D, Auluck S, Kityk IV, Kamarudin H (2011) Structural properties and bonding nature of 3-methyl-4-phenyl-5-(2-pyridyl)-1,2,4-triazole single crystal. Mater Chem Phys 130(1–2): 458–465
19. Irfan A (2014) First principle investigations to enhance the charge transfer properties by bridge elongation. J Theor Comput Chem 13(02):1450013

20. Muhammad S, Irfan A, Shkir M, Chaudhry AR, Kalam A, AlFaify S, Al-Sehemi AG, Al-Salami AE, Yahia IS, Xu HL, Su ZM (2014) How does hybrid bridging core modification robust the nonlinear optical properties in donor-π-acceptor configuration? a case study of dinitrophenol derivatives. J Comput Chem. doi:10.1002/jcc.23777
21. Irfan A, Al-Sehemi AG, Al-Assiri MS (2013) Modeling of multifunctional donor-bridge-acceptor 4, 6-di (thiophen-2-yl) pyrimidine derivatives: A first principles study. J Mol Graphics Modell 44:168–176
22. Irfan A, Jin R, Al-Sehemi AG, Asiri AM (2013) Quantum chemical study of the donor-bridge-acceptor triphenylamine based sensitizers. Spectrochim Acta A Mol Biomol Spectrosc 110:60–66
23. Irfan A (2014) Influence of the substitution on the electronic properties of perylene-3, 4: 9, 10-bis (dicarboximides): density functional theory study. Bull Chem Soc Ethiop 28(1):101–110
24. Irfan A, Ijaz F, Al-Sehemi A, Asiri A (2012) Quantum chemical approach toward rational designing of highly efficient oxadiazole based oligomers used in organic field effect transistors. J Comput Electron 11(4):374–384
25. Katz EH (1997) Organic molecular solids as thin film transistor semiconductors. J Mater Chem 7(3):369–376
26. Horowitz G, Hajlaoui ME (2000) Mobility in polycrystalline oligothiophene field-effect transistors dependent on grain size. Adv Mater 12(14):1046–1050
27. Newman CR, Frisbie CD, da Silva Filho DA, Brédas J-L, Ewbank PC, Mann KR (2004) Introduction to organic thin film transistors and design of n-channel organic semiconductors. Chem Mater 16(23): 4436–4451
28. Nakano M, Shinamura S, Houchin Y, Osaka I, Miyazaki E, Takimiya K (2012) Angular-shaped naphthodifurans, naphtho[1,2-b;5,6-b']- and naphtho[2,1-b;6,5-b']-difuran: are they isoelectronic with chrysene? Chem Commun 48(45):5671–5673
29. Tang CW, VanSlyke SA (1987) Organic electroluminescent diodes. Appl Phys Lett 51(12):913–915
30. Ho PKH, Kim J-S, Burroughes JH, Becker H, Li SFY, Brown TM, Cacialli F, Friend RH (2000) Molecular-scale interface engineering for polymer light-emitting diodes. Nature 404(6777):481–484
31. Al-Sehemi AG, Irfan A, Asiri AM (2014) Red and yellow color aspects of compound 3-dicyclopropylmethylene-5-dicyanomethylene-4-diphenylmethylenetetrahydrofuran-2-one chromism effect. Chin Chem Lett 25(4):609–612
32. Padinger F, Rittberger RS, Sariciftci NS (2003) Effects of postproduction treatment on plastic solar cells. Adv Funct Mater 13(1):85–88
33. Irfan A (2013) Quantum chemical investigations of electron injection in triphenylamine-dye sensitized TiO2 used in dye sensitized solar cells. Mater Chem Phys 142(1):238–247
34. Wrackmeyer MS, Hein M, Petrich A, Meiss J, Hummert M, Riede MK, Leo K (2011) Dicyanovinyl substituted oligothiophenes thermal stability, mobility measurements, and performance in photovoltaic devices. Sol Energy Mater Sol Cells 95(12):3171–3175
35. Irfan A, Nadeem M, Athar M, Kanwal F, Zhang J (2011) Electronic, optical and charge transfer properties of α, α'-bis(dithieno[3,2-b:2', 3'- d]thiophene) (BDT) and its heteroatom-substituted analogues. Comput Theor Chem 968(1–3):8–11
36. Irfan A, Al-Sehemi AG, Muhammad S, Zhang J (2011) Packing effect on the transfer integrals and mobility in α, α'-bis(dithieno[3, 2-b:2',3'-d]thiophene) (BDT) and its heteroatom-substituted analogues. Aust J Chem 64(12):1587–1592
37. Das S, Senanayak SP, Bedi A, Narayan KS, Zade SS (2011) Synthesis and charge carrier mobility of a solution-processable conjugated copolymer based on cyclopenta[c]thiophene. Polymer 52(25):5780–5787
38. Letizia JA, Cronin S, Ortiz RP, Facchetti A, Ratner MA, Marks TJ (2010) Phenacyl–thiophene and quinone semiconductors designed for solution processability and air-stability in high mobility n-channel field-effect transistors. Chem Eur J 16(6):1911–1928
39. Buonocore F, Matteo A (2009) Energetic of molecular interface at metal-organic heterojunction: the case of thiophenethiolate chemisorbed on Au(111). Theor Chem Acc 124(3–4):217–223
40. Wu Q-X, Geng Y, Liao Y, Tang X-D, Yang G-C, Su Z-M (2012) Theoretical studies of the effect of electron-withdrawing dicyanovinyl group on the electronic and charge-transport properties of fluorene-thiophene oligomers. Theor Chem Acc 131(3):1–9
41. Unni KNN, Dabos-Seignon S, Nunzi J-M (2006) Influence of the polymer dielectric characteristics on the performance of a quaterthiophene organic field-effect transistor. J Mater Sci 41(2): 317–322
42. Pingel P, Zen A, Neher D, Lieberwirth I, Wegner G, Allard S, Scherf U (2009) Unexpectedly high field-effect mobility of a soluble, low molecular weight oligoquaterthiophene fraction with low polydispersity. Appl Phys A 95(1):67–72
43. Koezuka H, Tsumura A, Ando T (1987) Field-effect transistor with polythiophene thin film. Synth Met 18(1–3):699–704
44. Mikhailov IA, Belfield KD, Masunov AE (2009) DFT-based methods in the design of Two-photon operated molecular switches. J Phys Chem A 113(25):7080–7089
45. Irfan A, Al-Sehemi AG, Muhammad S (2014) Push-pull effect on the charge transport properties in anthra [2, 3-b] thiophene derivatives used as dye-sensitized and hetero-junction solar cell materials. Synth Met 190:27–33
46. Irfan A, Al-Sehemi AG, Al-Assiri MS (2014) The effect of donors–acceptors on the charge transfer properties and tuning of emitting color for thiophene, pyrimidine and oligoacene based compounds. J Fluorine Chem 157:52–57
47. Irfan A, Chaudhry AR, Al-Sehemi AG, Al-Asiri MS, Muhammad S, Kalam A (2014) Investigating the effect of acene-fusion and trifluoroacetyl substitution on the electronic and charge transport properties by density functional theory. J Saudi Chem Soc. doi:10.1016/j.jscs.2014.09.009 (0)
48. Irfan A (2014) Highly efficient renewable energy materials benzo[2, 3-b]thiophene derivatives: electronic and charge transfer properties study Optik. Int J Light Electron Optics 125(17):4825–4830
49. Irfan A, Al-Sehemi AG, Al-Assiri MS (2014) Push–pull effect on the electronic, optical and charge transport properties of the benzo[2,3-b]thiophene derivatives as efficient multifunctional materials. Comput Theor Chem 1031:76–82
50. Irfan A (2014) Modeling of efficient charge transfer materials of 4,6-di(thiophen-2-yl)pyrimidine derivatives quantum chemical investigations computational. Mater Sci 81:488–492
51. Miyata Y, Nishinaga T, Komatsu K (2005) Synthesis and structural, electronic, and optical properties of oligo(thienylfuran)s in comparison with oligothiophenes and oligofurans. J Org Chem 70(4):1147–1153
52. Miyata Y, Terayama M, Minari T, Nishinaga T, Nemoto T, Isoda S, Komatsu K (2007) Synthesis of oligo(thienylfuran)s with thiophene rings at both ends and their structural, electronic, and field-effect properties. Chem–Asian J 2(12):1492–1504
53. Gidron O, Dadvand A, Sheynin Y, Bendikov M, Perepichka DF (2011) Towards "green" electronic materials. α-oligofurans as semiconductors. Chem Commun 47(7):1976–1978
54. Wu C-C, Hung W-Y, Liu T-L, Zhang L-Z, Luh T-Y (2003) Hole-transport properties of a furan-containing oligoaryl. J Appl Phys 93(9):5465–5471
55. Kadac K, Bosiak MJ, Nowaczyk J (2012) Synthesis and AC impedance studies of 2,6-distyrylbenzofuro[5,6-b]furan based new organic semiconductor. Synth Met 162(21–22):1981–1986
56. Nakano M, Niimi K, Miyazaki E, Osaka I, Takimiya K (2012) Isomerically pure anthra[2,3-b:6,7-b']-difuran (anti-ADF), −dithiophene (anti-ADT), and -diselenophene (anti-ADS): selective synthesis electronic structures, and application to organic field-effect transistors. J Org Chem 77(18):8099–8111
57. Niimi K, Mori H, Miyazaki E, Osaka I, Kakizoe H, Takimiya K, Adachi C (2012) [2,2[prime or minute]]Bi[naphtho[2,3-b]furanyl]: a

versatile organic semiconductor with a furan-furan junction. Chem Commun 48(47):5892–5894
58. Watanabe M, Su W-T, Chang YJ, Chao T-H, Wen Y-S, Chow TJ (2013) Solution-processed optoelectronic properties of functionalized anthradifuran. Chem–Asian J 8(1):60–64
59. Chen H, Delaunay W, Li J, Wang Z, Bouit P-A, Tondelier D, Geffroy B, Mathey F, Duan Z, Réau R, Hissler M (2013) Benzofuran-fused phosphole: synthesis electronic, and electroluminescence properties. Org Lett 15(2):330–333
60. Mitsudo K, Harada J, Tanaka Y, Mandai H, Nishioka C, Tanaka H, Wakamiya A, Murata Y, Suga S (2013) Synthesis of hexa(furan-2-yl)benzenes and their π-extended derivatives. J Org Chem 78(6): 2763–2768
61. Mitsui C, Soeda J, Miwa K, Tsuji H, Takeya J, Nakamura E (2012) Naphtho[2,1-b:6,5-b']difuran a versatile motif available for solution-processed single-crystal organic field-effect transistors with high hole mobility. J Am Chem Soc 134(12):5448–5451
62. Ponce Ortiz R, Herrera H, Mancheño MJ, Seoane C, Segura JL, Mayorga Burrezo P, Casado J, López Navarrete JT, Facchetti A, Marks TJ (2013) Molecular and electronic-structure basis of the ambipolar behavior of naphthalimide–terthiophene derivatives: implementation in organic field-effect transistors chemistry. A Eur J 19(37):12458–12467
63. Chaudhry AR, Ahmed R, Irfan A, Shaari A, Al-Sehemi AG (2013) Quantum chemical approach toward the electronic, photophysical and charge transfer properties of the materials used in organic field-effect transistors. Mater Chem Phys 138(2–3):468–478
64. Chaudhry AR, Ahmed R, Irfan A, Shaari A, Al-Sehemi AG (2014) Effects of electron withdrawing groups on transfer integrals, mobility, electronic and photo-physical properties of naphtho[2,1-b:6,5-b']difuran derivatives: a theoretical study. Sci Adv Mater 6(8): 1727–1739
65. Chaudhry AR, Ahmed R, Irfan A, Shaari A, Maarof H, Al-Sehemi AG (2014) First principles investigations of electronic, photoluminescence and charge transfer properties of the naphtho[2,1-b:6,5-b']difuran and its derivatives for OFET. Sains Malays 43(6): 867–875
66. Chaudhry AR, Ahmed R, Irfan A, Muhammad S, Shaari A, Al-Sehemi AG (2014) Effect of heteroatoms substitution on electronic, photophysical and charge transfer properties of naphtha [2,1-b:6,5-b'] difuran analogues by density functional theory. Comput Theor Chem 1045:123–134
67. Chaudhry AR, Ahmed R, Irfan A, Muhammad S, Shaari A, Al-Sehemi AG (2014) Influence of push-pull configuration on the electro-optical and charge transport properties of novel naphthodifuran derivatives: a DFT study. RSC Adv 4(90):48876–48887
68. Becke AD (1993) Density-functional thermochemistry III. The role of exact exchange. J Chem Phys 98(7):5648–5652
69. Lee C, Yang W, Parr RG (1988) Development of the Colle-Salvetti correlation-energy formula into a functional of the electron density. Phys Rev B 37(2):785–789
70. Hehre WJ, Ditchfield R, Pople JA (1972) Self-consistent molecular orbital methods XII. Further extensions of gaussian-type basis sets for Use in molecular orbital studies of organic molecules. J Chem Phys 56(5):2257–2261
71. Hariharan PC, Pople JA (1973) The influence of polarization functions on molecular orbital hydrogenation energies Theoretica. Chim Acta 28(3):213–222
72. Dill JD, Pople JA (1975) Self-consistent molecular orbital methods. XV extended gaussian-type basis sets for lithium, beryllium, and boron. J Chem Phys 62(7):2921–2923
73. Bauernschmitt R, Ahlrichs R (1996) Treatment of electronic excitations within the adiabatic approximation of time dependent density functional theory. Chem Phys Lett 256(4–5):454–464
74. Stratmann RE, Scuseria GE, Frisch MJ (1998) An efficient implementation of time-dependent density-functional theory for the calculation of excitation energies of large molecules. J Chem Phys 109(19):8218–8224
75. Van Caillie C, Amos RD (1999) Geometric derivatives of excitation energies using SCF and DFT. Chem Phys Lett 308(3–4):249–255
76. Van Caillie C, Amos RD (2000) Geometric derivatives of density functional theory excitation energies using gradient-corrected functionals. Chem Phys Lett 317(1–2):159–164
77. Furche F, Ahlrichs R (2002) Adiabatic time-dependent density functional methods for excited state properties. J Chem Phys 117(16): 7433–7447
78. Casida ME, Jamorski C, Casida KC, Salahub DR (1998) Molecular excitation energies to high-lying bound states from time-dependent density-functional response theory:characterization and correction of the time-dependent local density approximation ionization threshold. J Chem Phys 108(11):4439–4449
79. Gruhn NE, da Silva Filho DA, Bill TG, Malagoli M, Coropceanu V, Kahn A, Brédas J-L (2002) The vibrational reorganization energy in pentacene: molecular influences on charge transport. J Am Chem Soc 124(27):7918–7919
80. Reimers JR (2001) A practical method for the use of curvilinear coordinates in calculations of normal-mode-projected displacements and duschinsky rotation matrices for large molecules. J Chem Phys 115(20):9103–9109
81. Irfan A, Cui R, Zhang J (2009) Fluorinated derivatives of mer-Alq3: energy decomposition analysis, optical properties, and charge transfer study. Theor Chem Acc 122(5–6):275–281
82. Coropceanu V, Nakano T, Gruhn NE, Kwon O, Yade T, K-i K, Brédas J-L (2006) Probing charge transport in π-stacked fluorene-based systems. J Phys Chem B 110(19):9482–9487
83. Li Y, Zou L-Y, Ren A-M, Feng J-K (2012) Theoretical study on the electronic structures and photophysical properties of a series of dithienylbenzothiazole derivatives. Comput Theor Chem 981:14–24
84. Frisch MJ, Trucks GW, Schlegel HB, Scuseria GE, Robb MA, Cheeseman JR, Scalmani G, Barone V, Mennucci B, Petersson GA, Nakatsuji H, Caricato M, Li X, Hratchian HP, Izmaylov AF, Bloino J, Zheng G, Sonnenberg JL, Hada M, Ehara M, Toyota K, Fukuda R, Hasegawa J, Ishida M, Nakajima T, Honda Y, Kitao O, Nakai H, Vreven T, Jr, Peralta JE, Ogliaro F, Bearpark M, Heyd JJ, Brothers E, Kudin KN, Staroverov VN, Kobayashi R, Normand J, Raghavachari K, Rendell A, Burant JC, Iyengar SS, Tomasi J, Cossi M, Rega N, Millam JM, Klene M, Knox JE, Cross JB, Bakken V, Adamo C, Jaramillo J, Gomperts R, Stratmann RE, Yazyev O, Austin AJ, Cammi R, Pomelli C, Ochterski JW, Martin RL, Morokuma K, Zakrzewski VG, Voth GA, Salvador P, Dannenberg JJ, Dapprich S, Daniels AD, Farkas, Foresman JB, Ortiz JV, Cioslowski J, Fox DJ (2009) Gaussian 09 Revision A.02. Gaussian Inc, Wallingford
85. Zhang Y, Cai X, Bian Y, Li X, Jiang J (2008) Heteroatom substitution of oligothienoacenes: from good p-type semiconductors to good ambipolar semiconductors for organic field-effect transistors. J Phys Chem C 112(13):5148–5159
86. Marcus RA (1993) Electron transfer reactions in chemistry theory and experiment. Rev Mod Phys 65(3):599–610
87. Brédas JL, Calbert JP, da Silva Filho DA, Cornil J (2002) Organic semiconductors: a theoretical characterization of the basic parameters governing charge transport. Proc Natl Acad Sci 99(9):5804–5809
88. Shinamura S, Osaka I, Miyazaki E, Nakao A, Yamagishi M, Takeya J, Takimiya K (2011) Linear- and angular-shaped naphthodithiophenes: selective synthesis properties, and application to organic field-effect transistors. J Am Chem Soc 133(13):5024–5035
89. Mohakud S, Alex AP, Pati SK (2010) Ambipolar charge transport in α-oligofurans: a theoretical study. J Phys Chem C 114(48):20436–20442
90. Yi Y, Zhu L, Brédas J-L (2012) Charge-transport parameters of acenedithiophene crystals: realization of one-, two-, or three-dimensional transport channels through alkyl and phenyl derivatizations. J Phys Chem C 116(8):5215–5224

91. Politzer P, Truhlar (Eds.) DG (1981) Chemical applications of atomic and molecular electrostatic potentials. Plenum, New York
92. Stewart RF (1979) On the mapping of electrostatic properties from bragg diffraction data. Chem Phys Lett 65(2):335–342
93. Murray JS, Politzer P (2011) The electrostatic potential: an overview. Mol Sci 1(2):153–163
94. Shkir M, Muhammad S, AlFaify S, Irfan A, Yahia IS (2015) A dual approach to study the electro-optical properties of a noncentrosymmetric l-asparagine monohydrate. Spectrochim Acta A Mol Biomol Spectrosc 137:432–441
95. Muhammad S, Xu H, Janjua MRSA, Su Z, Nadeem M (2010) Quantum chemical study of benzimidazole derivatives to tune the second-order nonlinear optical molecular switching by proton abstraction. Phys Chem Phys 12(18):4791–4799
96. Irfan A, Zhang J, Chang Y (2010) Theoretical investigations of the charge transfer properties of anthracene derivatives. Theor Chem Acc 127(5–6):587–594
97. Irfan A, Zhang J (2009) Effect of one ligand substitution on charge transfer and optical properties in mer-Alq3: a theoretical study. Theor Chem Acc 124(5–6):339–344